The Effect of Molecular Shape and Microphase Segregation on the Formation of Liquid Crystal Phases in Poly-Ols

Jonathan J. West [a] , Guenola Bonsergent [a] , Grahame Mackenzie [a] , David F. Ewing [a] , John W. Goodby [a] , Thierry Benvegnu [b] , Daniel Plusquellec [b] , Sabrina Bachir [c] , Phillipe Bault [c] , Olivier Douillet [c] , Paul Godé [c] , Gerard Goethals [c] , Patrick Martin [c] & Pierre Villa [c]

[a] The School of Chemistry, The University of Hull, Hull, HU6 7RX, England

[b] Laboratoire de Chimie Organique et des Substances Naturelles, associé au CNRS, Ecole Nationale Supérieure de Chimie de Rennes, Avenue du Général Leclerc, 35700, Rennes, France

[c] Université de Picardie, Jules Verne, Faculté des Sciences, Laboratoire de Chimie Organique et Cinétique, 33 rue Saint Leu, 80039, Amiens, Cedex, France

PLEASE SCROLL DOWN FOR ARTICLE

The Effect of Molecular Shape and Microphase Segregation on the Formation of Liquid Crystal Phases in Poly-Ols

JONATHAN J. WEST[a], GUENOLA BONSERGENT[a],
GRAHAME MACKENZIE[a], DAVID F. EWING[a], JOHN W. GOODBY[a]*,
THIERRY BENVEGNU[b], DANIEL PLUSQUELLEC[b],
SABRINA BACHIR[c], PHILLIPE BAULT[c], OLIVIER DOUILLET[c],
PAUL GODÉ[c], GERARD GOETHALS[c], PATRICK MARTIN[c] and
PIERRE VILLA[c]

[a]*The School of Chemistry, The University of Hull, Hull HU6 7RX, England,* [b]*Laboratoire de Chimie Organique et des Substances Naturelles, associé au CNRS, Ecole Nationale Supérieure de Chimie de Rennes, Avenue du Général Leclerc, 35700 Rennes, France and* [c]*Université de Picardie, Jules Verne, Faculté des Sciences, Laboratoire de Chimie Organique et Cinétique, 33 rue Saint Leu – 80039, Amiens CEDEX, France*

In this article we examine the effect of molecular shape on the formation of thermotropic phases of alkyl-substituted poly-ols. The relationship between the cross-sectional area of the hydrophilic head group with respect to the that of the hydrophilic tails determines the type of mesophase formed. The results obtained are similar to those found for the formation of lyotropic phases.

1. INTRODUCTION

In classical, non-amphiphilic, thermotropic liquid crystal systems, it is common to develop property/structure correlations *via* the investigation of the variation in transition temperature(s) as a function of systematic changes in molecular structure[1-3]. Usually, it is found that the clearing points and liquid crystal to liquid crystal transition temperatures are extremely sensitive to small structural

---

* Corresponding Author: e-mail: J.W.Goodby@chem.hull.ac.uk

Effect of Fluoro-substitution on the Formation of Smectic C phases

C$_6$H$_{11}$—⬡—⬡—⬡—OC$_6$H$_{13}$

SmB 216 • SmA 228.5 • Iso Liq

F
C$_6$H$_{11}$—⬡—⬡—⬡—OC$_6$H$_{13}$

G 176 • SmA 210 • Iso Liq

F
C$_6$H$_{11}$—⬡—⬡—⬡—OC$_6$H$_{13}$

SmC 131.5 • N 166.5 • Iso Liq

F
C$_6$H$_{11}$—⬡—⬡—⬡—OC$_6$H$_{13}$

G 78 • SmB 92 • SmI 93 • SmC 118 • SmA 115 • N 166.5 • Iso Liq

F F
C$_6$H$_{11}$—⬡—⬡—⬡—OC$_6$H$_{13}$

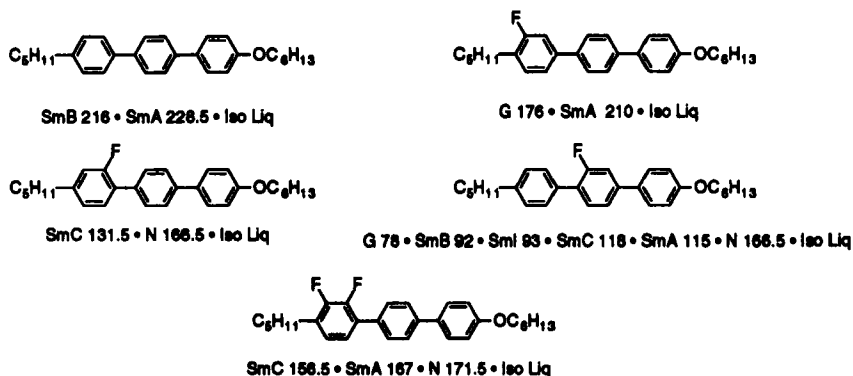**SmC 156.5 • SmA 167 • N 171.5 • Iso Liq**

FIGURE 1 The effect of lateral fluoro-substitution on mesophase formation and transition temperatures in some alkoxy-alkyl-terphenyls

changes at the molecular level, and, in fact, many studies have been made in relation to the effects of substituent size and position on mesophase formation and physical properties. The molecular design and engineering of liquid crystal materials for use in display devices takes property/structure correlations to the ultimate limit, where in many cases changing a single atom or a functional group in a selected molecular system can markedly affect the application and properties of a resulting material. For example, figure 1 shows the effect that the introduction, position and number of lateral fluoro-substituents has on mesophase formation and transition temperatures in fluoro-substituted 4-alkoxy-4-alkylterphenyls[4]. The position and number of fluoro-substituents are critical in determining whether or not the materials are suitable as hosts in ferroelectric mixtures for display applications. In a sense this is "sub-molecular" engineering, and is similar to how materials are examined in biological and pharmaceutical systems, *eg* protein-ligand interactions.

1

C$_n$H$_{2n+1}$O
C$_n$H$_{2n+1}$O—⬡—N—⬡—O—⬡—O—⬡—N—⬡—OC$_n$H$_{2n+1}$
OC$_n$H$_{2n+1}$

n = 11 Cr 144 SmC 146 °C Cub 163 Iso Liq
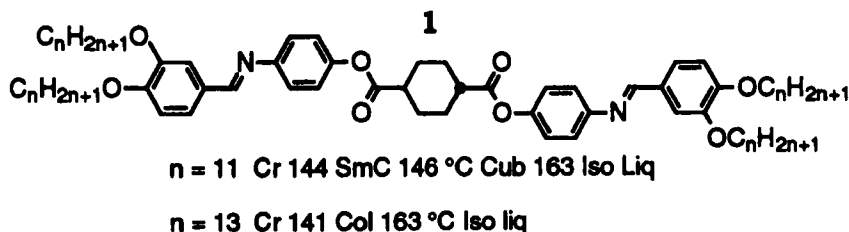
n = 13 Cr 141 Col 163 °C Iso liq

FIGURE 2 No Caption

This microscopic approach to the engineering of liquid-crystalline materials often ensures that the boundaries between rod-like (calamitic), disc-like (discoid) and spherical systems are not traversed. The one molecular template that has allowed examination of these interfaces is the phasmidic or polycatenar structure where multiple terminal chains induce molecular curvature which in turn enables columnar to lamellar phase transitions to occur[5]. The general structure **1**, in figure 2, gives two examples of a homologous series where the increasing proportional volume of the aliphatic chains affects the molecular shape and consequently the packing constraints of the molecules. The longer the chains the higher the degree of curvature that is introduced into the packing together of the molecular ensembles/clusters. As the curvature is increased the lamellar phases give way to cubic and then columnar modifications.
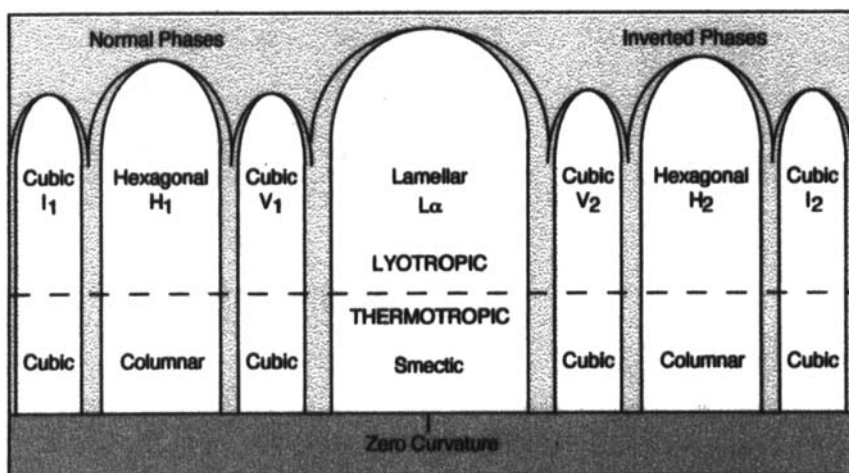
FIGURE 3

A more detailed view of the way that these phases are formed is to consider that the aliphatic chains of compounds of structure **1** act as a solvent with respect to the packing of the rigid aromatic cores. As the molecules pack together there is microphase segregation with the aliphatic portions of the molecules packing together separately from the aromatic regions. Where the two molecular segments have similar volumes, with respect to their cross-sectional areas, a layered mesophase will be formed. However, where there is a substantial difference at the interface between the two segregated regions, curvature will be introduced resulting in the formation of cubic and columnar mesophases[6]. A similar situation arises with lyotropic liquid crystals as the volume of the solvent is increased

the interfacial area between the solvent and the amphiphile changes so that again curvature is introduced. At zero curvature a lamellar phase is formed, but as the curvature is increased cubic then columnar phases are formed. Thus, there is a direct comparison between the effects of curvature in thermotropic and lyotropic systems, as shown in figure 3.
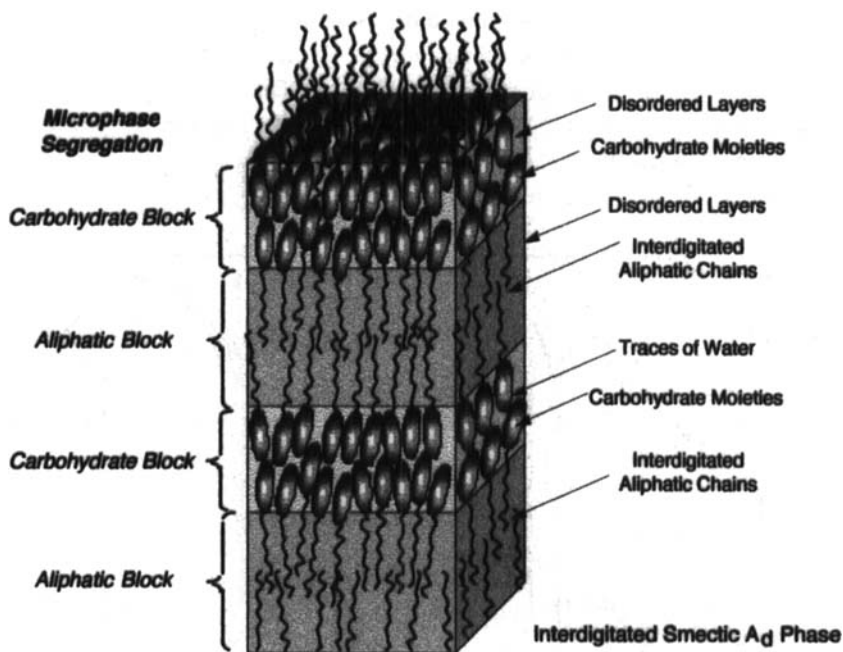
FIGURE 4 Microphase segregation to give a lamellar phase

Over the past few years we have been investigating the effects of molecular shape, flexibility and curvature in a variety of alkyl-substituted poly-ols, many of which were derived from acyclic sugar systems[7,8]. These materials were often found to exhibit both thermotropic and lyotropic phases, *ie* they are amphitropic liquid crystals. For systems that are composed of one aliphatic chain and one sugar/poly-ol head group, lamellar smectic A or A* phases were found to be formed through microphase segregation of the carbohydrate moieties with respect to the aliphatic chains, see figure 4.

Our early studies examined the effect on the clearing point of the thermotropic phases of alkyl-substituted poly-ols with respect to increasing the number of hydroxyl groups[8]. The liquid-crystalline phase behaviour of a variety of dodecyl substituted poly-ols was studied, see figure 5. It was found that the clearing

FIGURE 5 Comparison of the clearing point transition temperatures of a variety of dodecyl substituted poly-ols as a function of the number of hydroxyl groups
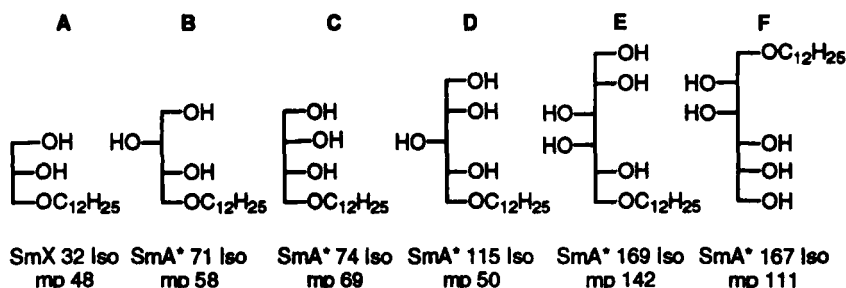
points varied linearly with respect to the number of hydroxyl groups in the head group of the amphiphile, see figure 6. No change in mesophase type (*ie* lamellar to columnar) was found which indicates that the head groups remain relatively linear and do not fold up into bulky intra-molecularly hydrogen bonded systems as the number of CH_2OH groups is increased across the series. Moreover, the results imply that there is a "quantifiable amount of thermal stability" for the mesophase that is introduced into the system per each CH_2OH group that is incorporated into the head group of the molecular structure.

In addition to showing a linear dependence of clearing point on the number of hydroxyl groups, it was also found that there was little or no effect of molecular chirality on the clearing points, compare for example compounds **B** and **C**, and, **E** and **F** in figure 5. In typical calamitic systems, molecular asymmetry can strongly affect mesophase behaviour, but in the case of amphiphiles it appears the effects of that molecular asymmetry have on the packing of the head groups (and molecules) together is lost in the general disordered microphase segregated band of hydroxylated head groups in the lamellar phase.

Following this study we reported the effects on the self-organising properties caused by the sequential movement of the position of a dodecyl chain in acyclic x-*O*-dodecyl-(D or L)-xylitols[7], **2**, see figure 7. The movement of the dodecyl chain from the terminal position to the inner positions 2 or 4 shown in figure 7 has the effect of increasing the bulky nature of the head group while at the same time reducing its internal flexibility.

The result is that the curvature has not been increased enough for columnar phases to appear, however, the stability of the lamellar phase is increased substantially. Movement of the dodecyl chain to the central position, 3, results in a material with a symmetrical head group, that is much more bulky and more likely to induce curvature than the linear system presented for the 1-position. Again no columnar or cubic phases are found, but there is a further increase in
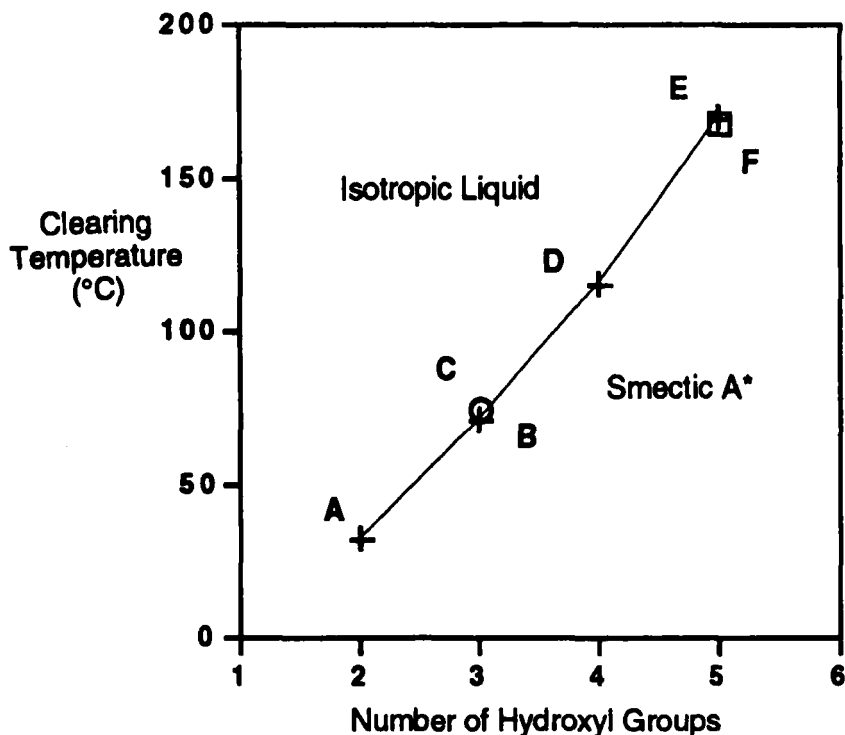
FIGURE 6 Clearing points (°C) of a variety of dodecyl substituted poly-ols (**A** to **F**) as a function of the number of hydroxyl groups (n)

mesophase stability. The increased stability of the mesophase is probably due to the increased rigidity of the head group. In addition to the clearing points rising, the melting points also increase across the series 1/5 < 2/4 < 3.

In order to develop systematic property/structure correlations further we investigated the effects of the linking group, **Z**, positioned between a sugar unit and the aliphatic chain in monosubstituted systems, on the lyotropic and thermotropic properties of poly-ols[8]. For this study of the self-organising behaviour of alkyl substituted xylitols, where the aliphatic chain was attached to the a xylitol moiety *via* either an ether, ester or thioether linkage, were investigated, see general structure **3** in figure 8. Combining our results on the thermotropic properties of the 1-*O*-alkanoyl-D or L-xylitols with those already available from Dahlhoff *et al*[9], we were able to show that the efficiency of the linking group in the formation of thermotropic phases follows the pattern[10],
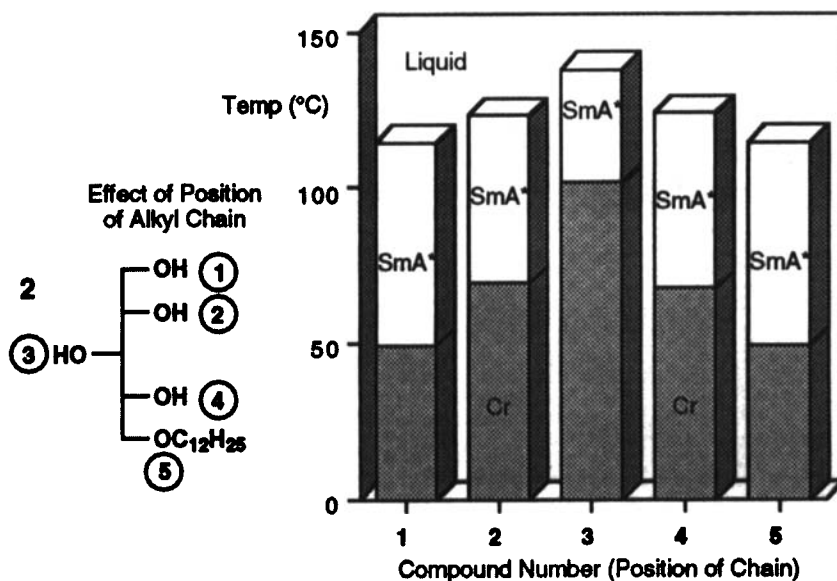
$$-SR > -OCOR > -OR$$

FIGURE 7 Effect of position on clearing temperatures in x-O-dodecyl-(D or L)-xylitols, 2

whereas, surprisingly, the reverse sequence appears to be the case for lyotropic phases. However, it should be emphasised that the effect of the nature and structural properties of the linking group positioned between the aliphatic chain and the sugar moiety does not markedly affect mesophase formation and stability, unlike the situation normally encountered for linking groups in conventional thermotropic materials.

In this present study, we investigated how the relative size and internal flexibility of the head group affects mesophase formation, in particular in terms of the competition to form lamellar versus columnar mesophases, ie we were engaged in searching for the point at which lamellar phases would give way to columnar phases as we increased the size and rigidity of the head group. For these studies we selected to examine systems 4 and 5 which could be compared with compounds of type 2. We see, particularly for the 3-substituted xylitol, 2, that the head group is forked, and therefore bulky, see figure 7. For this structure the head group can spread out to give a T-shaped gross molecular shape, ie it ought to be able to induce curvature as the cross-sectional area of the head group is much larger than that of the aliphatic chain, and as a consequence this shape should preferentially support columnar mesophase formation. However, in practice there appears to be enough flexibility associated with the branching point (for the
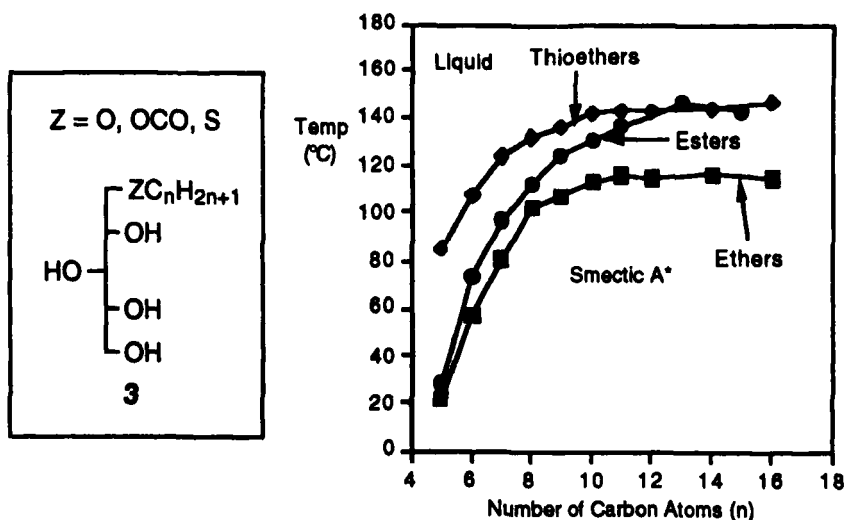
FIGURE 8 Effects of the linking group, Z, on the clearing points (°C) of alkyl substituted xylitols, where the aliphatic chain was attached to the a xylitol moiety *via* either an ether, ester or thioether linkage

two CHOH and CH_2OH groups) in the head group that there will be much dynamic motion and as a result the molecule can also appear to have a relatively linear structure. Thus we sought; (i) to make the head group relatively the same size but with much less flexibility thereby increasing its "effective" bulk (compounds of type **4**), and (ii) to extend the hydrophilic arms of the forked head group in order to increase its bulk whilst still retaining flexibility (compounds of type **5**)

Figure 9 shows computer simulations of compounds **2, 4** and **5** (the tetradecyl homologue, **5** (C14), was selected for study because it exhibits liquid-crystal properties over a wide temperature range). The simulations show how the cross-sectional area of the head group increases in size as a dodecyl chain is moved sequentially from one position to the next in the x-*O*-dodecyl-(D or L)-xylitols, **2** (top three structures). For compounds based on derivatives of tris (**4**) the head group has less freedom to move (fourth structure), and in compounds of type **5** the head group has been effectively doubled in size in comparison to compounds of type **2**.

In the following we report on the synthesis and characterization of compounds of structure **4**, and we present preliminary results for one example of the series compounds of general structure **5**.
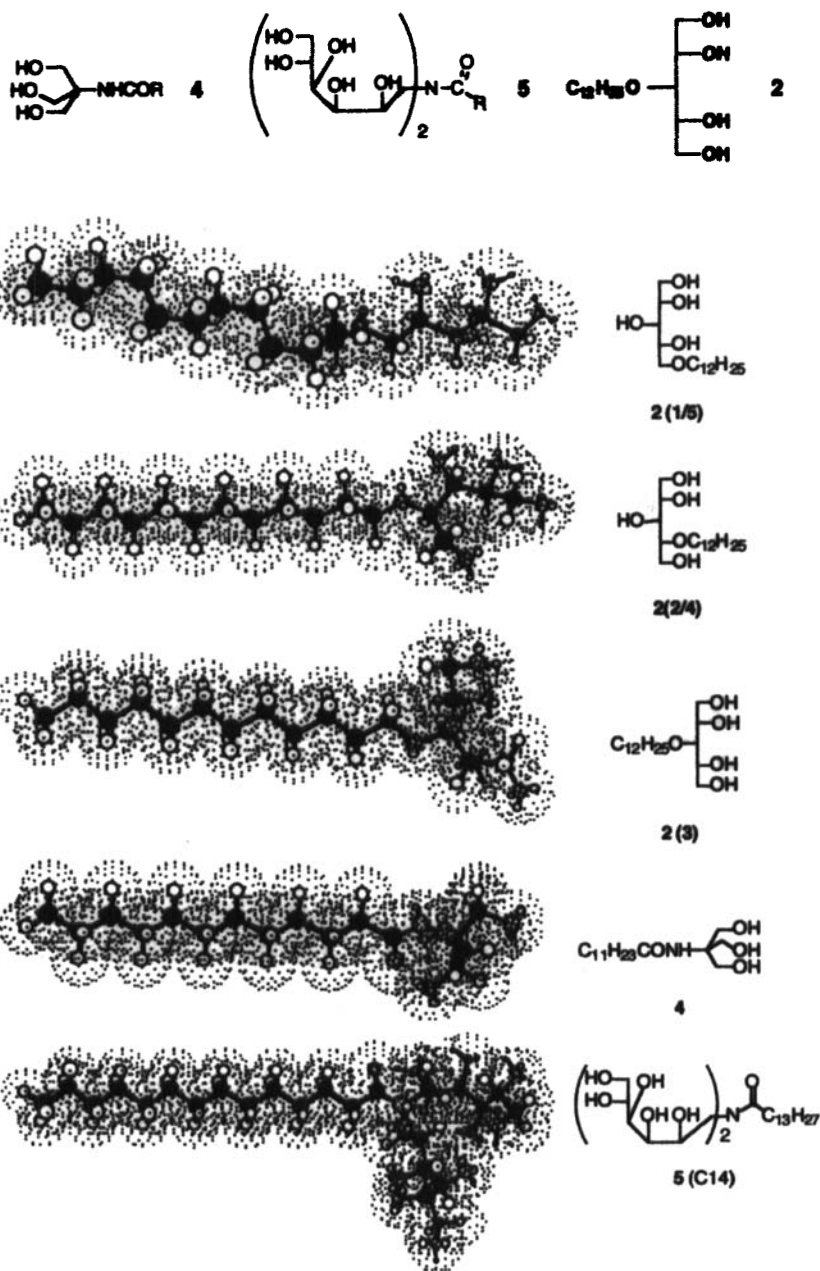
FIGURE 9 Minimised structures for the dodecyl and dodecanoyl compounds of type **2, 4** and **5** (C14)

TABLE I NMR Date for N-[2–hydroxy-1,1–*bis*-hidroxymethyl]ethylalkanamides, **4(a-m)**

ns (n) in chain	^1H NMR (DMSO)						
	CH_3 (3H, t)	CH_2 (m)	$OCCH_2\underline{CH}_2$ (2H, quint)	$OCCH_2$ (2H, t)	$HO\underline{CH}_2$ (6H, d)	OH (3H, t)	NH (
7	0.85	1.25	1.40	2.15	3.53	4.78	7
8	0.85	1.25	1.45	2.11	3.50	4.74	7
9	0.85	1.23	1.45	2.11	3.50	4.75	7
10	0.85	1.25	1.45	2.15	3.55	4.75	7
11	0.83	1.23	1.45	2.11	3.50	4.75	7
12	0.84	1.22	1.45	2.11	3.50	4.75	7
13	0.85	1.20	1.45	2.10	3.50	4.75	7
14	0.84	1.23	1.45	2.11	3.50	4.75	7
15	0.84	1.25	1.50	2.10	3.50	4.75	7
16	0.84	1.22	1.45	2.10	3.50	4.75	7
17	0.85	1.25	1.45	2.10	3.50	4.75	7
18	0.84	1.22	1.45	2.10	3.50	4.74	7
21	0.85	1.25	1.50	2.10	3.50	4.75	7

EXPERIMENTAL

The alkanoyl derivatives of tris, 7, *N*-[2-hydroxy-1,1-*bis*-hydroxymethyl]ethylalkanamides (**4a-m**) were prepared by the method shown in the scheme[11]. An example of the method is described for the octanoyl derivative (**4a**), all of the other homologues were prepared in the same way. Table I (NMR data) and Table II (CHN analyses) confirm the structures of the other homologues that were prepared.

RCOOH   +   (structure 7)   →   (structure 4(a-m))

6(a-m)   **7**   **4(a-m)**
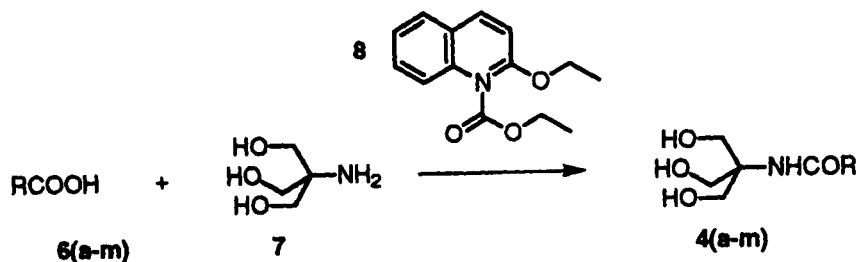
SCHEME

TABLE II Elemental Analyses for the *N*-[2–hydroxy-1,1–*bis*-hidroxymethyl]ethylalkanamides, 4(a-m)

Compd	Carbons (n) in chain	Calculated			Found		
	n	C	H	N	C	H	N
4a	7	58.27	10.19	5.66	58.09	10.39	5.59
4b	8	59.74	10.41	5.36	59.64	10.80	5.27
4c	9	61.06	10.61	5.09	60.88	10.94	4.96
4d	10	62.25	10.80	4.84	62.37	11.13	7.76
4e	11	63.33	10.96	4.62	63.20	11.31	4.51
4f	12	64.31	11.11	4.41	64.46	11.50	4.29
4g	13	65.22	11.25	4.23	65.25	11.54	4.04
4h	14	66.05	11.38	4.05	65.83	11.72	3.92
4i	15	66.81	11.49	3.90	66.75	11.91	3.74
4j	16	67.52	11.60	3.75	67.22	12.09	3.57
4k	17	68.17	11.70	3.61	68.29	12.04	3.33
4l	18	68.78	11.80	3.49	68.70	12.25	3.35
4m	21	70.38	12.04	3.16	70.36	12.43	2.82

Confirmation of the structures of the intermediates and final products was obtained by ^{1}H NMR spectroscopy (JEOL JNM-GX270 spectrometer), infra red spectroscopy (Perkin Elmer 783 spectrophotometer), mass spectroscopy (Finnigan-MAT 1020 GC/MS spectrometer) and CHN (Fisons EA 1108 CHN instrument). The progress of the reactions was frequently monitored using thin layer chromatography (Merck silica gel 60 F254). Phase identification and determination of phase transition temperatures were carried out by thermal polarised light microscopy using a Zeiss Universal polarising transmitted light microscope equipped with a Mettler FP52 microfurnace in conjunction with an FP50 central processor. Purification was achieved by high performance liquid chromatography using a Gilson 305 pump, 306 pump injection unit and a Dynamax 60Å amino column. Fractions were collected using a Gilson 202 fraction collector, Sedex 55 mass separation unit and Gilson 201–202 controller.
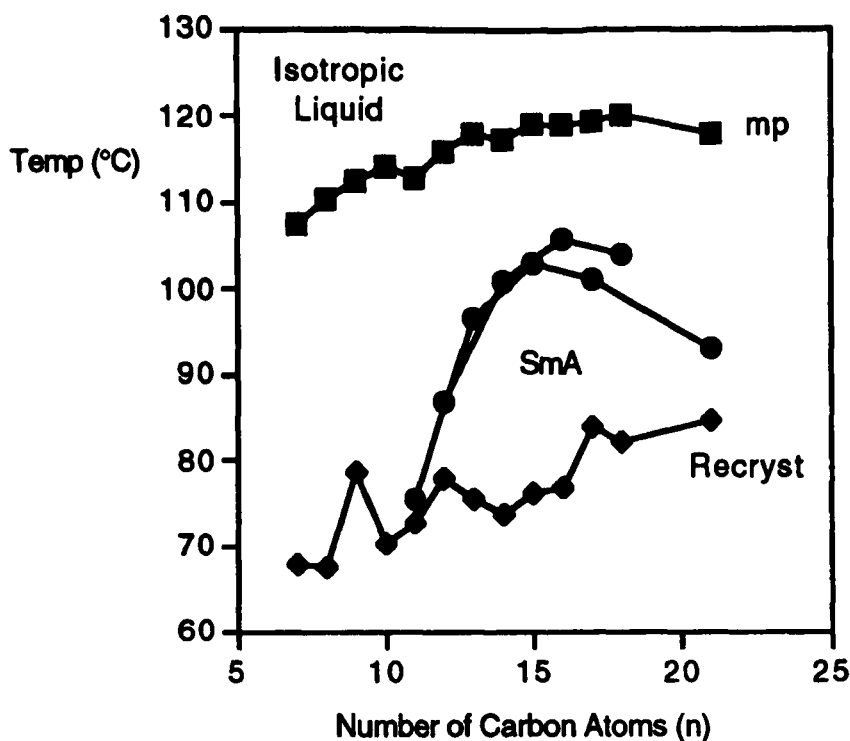

FIGURE 10 Transition temperatures (°C) as a function of chain length for compounds 4(a-m)

Differential Scanning Calorimetry was used to determine enthalpies of transition and to confirm the phase transition temperatures determined by optical

microscopy. Differential scanning thermograms (scan rate 10 min^{-1}) were obtained using a Perkin Elmer DSC 7PC system operating with UNIX software. The results obtained were standardised relative to indium (measured onset 156.68 C, Δ H 28.47 Jg^{-1})[12].
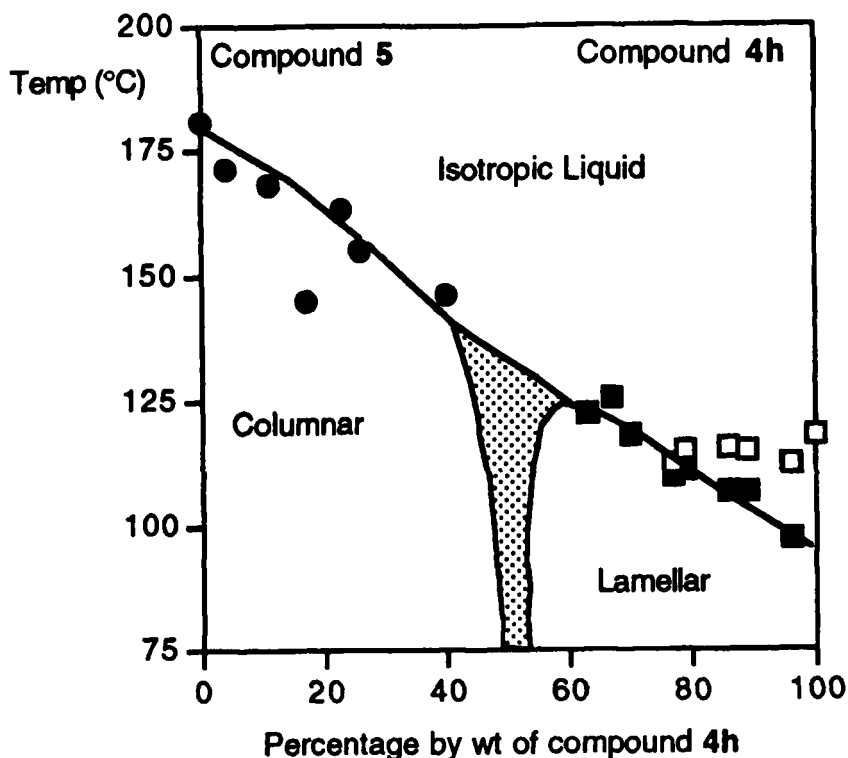

FIGURE 11 Miscibility phase diagram (wt %) as a function of temperature (°C) between compounds 5 (C14) and **4h**

Molecular modelling studies were performed on a Silicon Graphics workstation (Indigo XS24, 4000) using the programs Quanta and CHARMm. Within CHARMm, the Adopted Basis Newton Raphson (ABNR) algorithm was used to locate the molecular conformation with the lowest potential energy. The minimisation calculations were performed until the root mean square (RMS) force reached 4.184 kJ mol^{-1}Å^{-1}, which is close to the resolution limit. The RMS force is a direct measure of the tolerance applied to the energy gradient (*ie*, the rate of change of potential energy with step number) during each cycle of minimisation. The calculation was terminated in cases where the average energy gra-

dient was less than the specified value. The results of the molecular mechanics calculations were generated using the programs QUANTA V4.0 and CHARMm V22.2. The programs were developed and integrated by Molecular Simulations Inc. The modelling packages assume the molecules to be a collection of hard particles held together by elastic forces, in the gas phase, at absolute zero, in an ideal motionless state, and the force fields used are those described in CHARMm V 22.2.

Synthetic procedure for N-[2-hydroxy-1,1-bis-hydroxymethyl] ethyloctanamide (4a)

A mixture of tris(hydroxymethyl) aminomethane (7.05 g, 58 mmol), **7**, octanoic acid (10.0 g, 63 mmol), **6a**, and EEDQ (16.87 g, 68 mmol), **8**, in absolute ethanol (250 ml) was heated under reflux for 7 h. The mixture was cooled and the resulting white precipitate was filtered, washed with cold diethyl ether and dried in air. The white solid was recrystallised in acetonitrile (250 ml) by soxlet extraction and cooled, to yield white needles that were filtered, washed with cold diethyl ether and dried in *vacuo*. Yield 4.32 g, 25%.

Transition Temperatures and Enthalpies

The melting behaviour of the materials was examined using transmitted polarized light microscopy for the clearing points (cl pts) and differential scanning calorimetry for the melting (mps) and recrystallization (recryst) points. The enthalpies, ΔH, of all of the phase transitions were also evaluated from differential scanning calorimetry. The results obtained from both of the techniques of study are shown together in Table III, and the transition temperatures are plotted as a function of aliphatic chain length in figure 10. The results show that liquid crystal phases are only observed for the dodecanoyl and higher homologues, and for all of these materials the liquid crystal phases are monotropic. For the shorter homologues, liquid crystallinity is not observed simply because the melting points are too high and the supercooling of the crystal state is too small. Thus for these materials the liquid crystal phase behaviour must be considered as virtual. Nevertheless, there are some interesting trends that can be deduced from Table III. Firstly as the chain is extended the clearing transition temperatures rise almost linearly, the clearing temperatures then level off and fall. Thus the most stable liquid crystal phases occur at around 14 to 16 carbon atoms in the aliphatic chain. Similarly, the enthalpy values for the clearing point, like the transition temperatures, rise as the aliphatic chain length reaches 14 to 16 carbon atoms in length. For the shorter homologues there is virtually no odd-even effect, whereas

for the higher homologues the alternation effects are quite pronounced. Secondly, the melting points are almost constant with respect to chain length. Thirdly, the steep rise in the stability of the liquid crystal phase starting at the dodecanoyl homologue suggests that the shorter homologues exhibit only weak tendencies to form mesophases. Figure 10 shows these trends as a function of terminal aliphatic chain length.

TABLE III Transition Temperatures (C) and Enthalpies ΔH [kJmol^{-1}] for Compounds 4(a-m)

Compd	n	Cr		SmA		Isotropic Liquid	Recrystallisation
4a	7	•	107.4	-	-	•	67.9
	ΔH		[42.35]				[35.11]
4b	8	•	110.2	-	-	•	67.7
	ΔH		[44.74]				[37.17]
4c	9	•	112.5	-	-	•	78.8
	ΔH		[49.11]				[42.86]
4d	10	•	114.0	-	-	•	70.5
	ΔH		[51.26]				[43.48]
4e	11	•	112.8	(•	75.6)	•	72.9
	ΔH		[51.46]		[0.78]		[43.72]
4f	12	•	115.9	(•	86.7)	•	78.2
	ΔH		[55.25]		[1.42]		[48.55]
4g	13	•	118.1	(•	96.6)	•	75.5
	ΔH		[59.89]		[1.34]		[31.70]
4h	14	•	117.2	(•	100.9)	•	73.9
	ΔH		[60.57]		[1.31]		[51.89]
4i	15	•	118.9	(•	102.9)	•	76.2
	ΔH		[65.94]		[1.23]		[49.56]
4j	16	•	119.0	(•	105.8)	•	77.0
	ΔH		[68.64]		[1.16]		[55.83]
4k	17	•	119.4	(•	101.0)	•	84.1
	ΔH		[67.17]		[0.68]		[59.85]
4l	18	•	120.0	(•	103.9)	•	82.3
	ΔH		[71.74]		[0.78]		[64.11]
4m	21	•	118.0	(•	93.1)	•	84.6
	ΔH		[72.70]		[0.57]		[60.94]

Phase Characterisation

The mesophases exhibited by all of the compounds were determined by co-miscibility within the series to be of the same type. Thus, the materials exhibit a single liquid crystal phase. Classification was achieved in two ways; firstly from observations of the defect textures exhibited by the mesophase on cooling from

the isotropic liquid, and secondly through miscibility studies with a standard material.

The defect textures exhibited by the mesophase fall into three categories. On untreated clean glass substrates focal-conic, oily streak and homeotropic defect textures were observed. The presence of focal-conic defects, characterised by elliptical and hyperbolic lines of optical discontinuity, and homeotropic alignment in various specimens is diagnostic for the presence of a smectic A phase. Plate 1 shows the focal-conic texture of the smectic A phase of *N*-[2-hydroxy-1,1-*bis*-hydroxymethyl]ethyltetradecanamide (**4g**). Miscibility studies with decyl β-D-glucopyranoside[13], which is a standardised carbohydrate that exhibits smectic A^*_d phase, confirmed the above hypothesis for the classification of the liquid crystal phase.
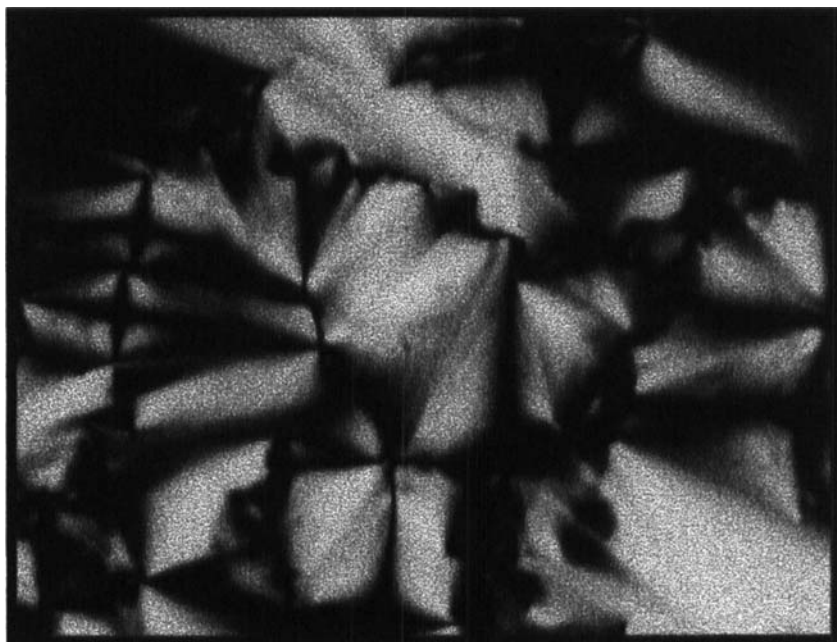
PLATE 1 The focal-conic texture of the smectic A phase of *N*-[2-hydroxy-1,1-*bis*-hydroxyme-thyl]ethyltetradecanamide (**4g**) (×100)

Thus, the phase exhibited by the materials is, not surprisingly, found to be smectic A that has a speculated structure similar to the one shown in figure 4. In this microphase segregated structure the aliphatic chains in adjacent pairs of layers are expected to partially interdigitate. The carbohydrate moieties, on the other
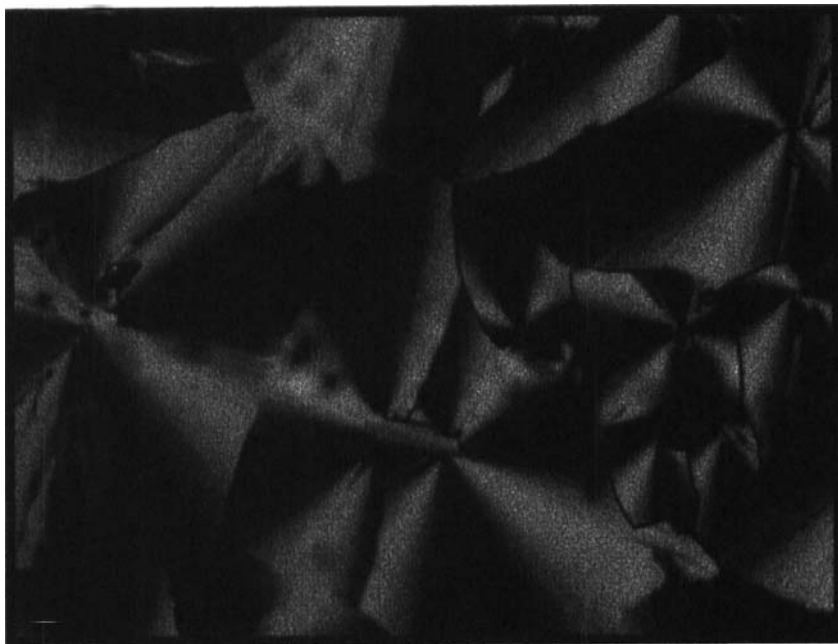
PLATE 2 The fan texture of the columnar phase of *N,N-bis*-(D-mannitolyl)tetradecylamide **5** (C14)(x100)

hand, are expected to be arranged on the peripheral surfaces of the bilayer structure, and thus the resulting structure resembles that of a membrane. The mesophase could, therefore, be classified as an interdigitated bilayer structure, and as the stronger intermolecular interactions are at the surfaces of the bilayer ordering, the structure could be said to be inverted relative to that normally found for the smectic A phase where the strong interactions are more likely to be found within the layer. Thus, the proposed structure for the mesophase is in keeping with structures reported for similar phases of carbohydrate liquid crystals, thus this would classify the mesophase as smectic A_d.

N,N-Bis-(D-mannitolyl)tetradecylamide 5 (C14)

N,N-Bis-(D-mannitolyl)tetradecylamide was synthesised (as an example of series **5**), as noted, to increase the number and extend the length of the hydroxylated chains in the head group[14]. The synthesis of this of this material and related homologues will be reported elsewhere. However, for the purposes of this study
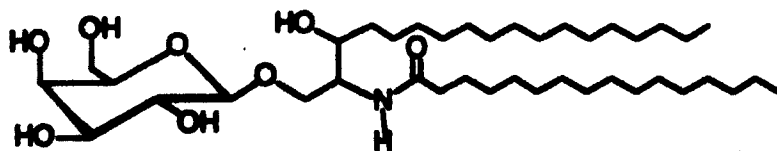
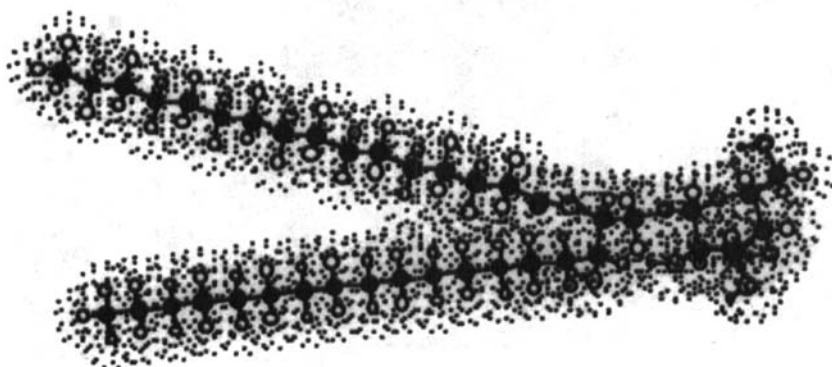R = C₁₇H₃₅   Crystal 91.3 Columnar 193.2 °C isotropic Liquid   6

FIGURE 12 Structure and phase transitions for octadecyanoyl D,L-dihydrogalactocerebroside, **6**

it is useful to include the preliminary results that we have obtained on the dodecylamide.

This material was found to exhibit the following phase behaviour:

Crystal 147.71 columnar 180.55 isotropic liquid, recrystallization 20.84°C

The compound, unlike those discussed previously, appears to have a large enough head group to induce the formation of a columnar mesophase. The mesophase formed from the isotropic liquid on cooling, showed no tendency to form a homeotropic texture, nor did it exhibit focal-conic defects. Instead a fan texture, typical of a columnar phase, was formed, see plate 2.

Mixture studies between *N,N-bis*-(D-mannitolyl)tetradecylamide **5** (C14) and the tris compounds **4** showed a gap in the middle of the phase diagram indicating that the mesophases of two compounds are immiscible, see figure 11. Although immiscibility is not a proof that the two mesophases have separate identities, in this case the fact that the isotropization line appears to be continuous except for the gap in the centre supports the view that the two phases are different.

In order to investigate further the nature of the liquid-crystalline phase of compound **6** we decided to examine binary mixtures of *N,N-bis*-(D-mannitolyl)tetra-
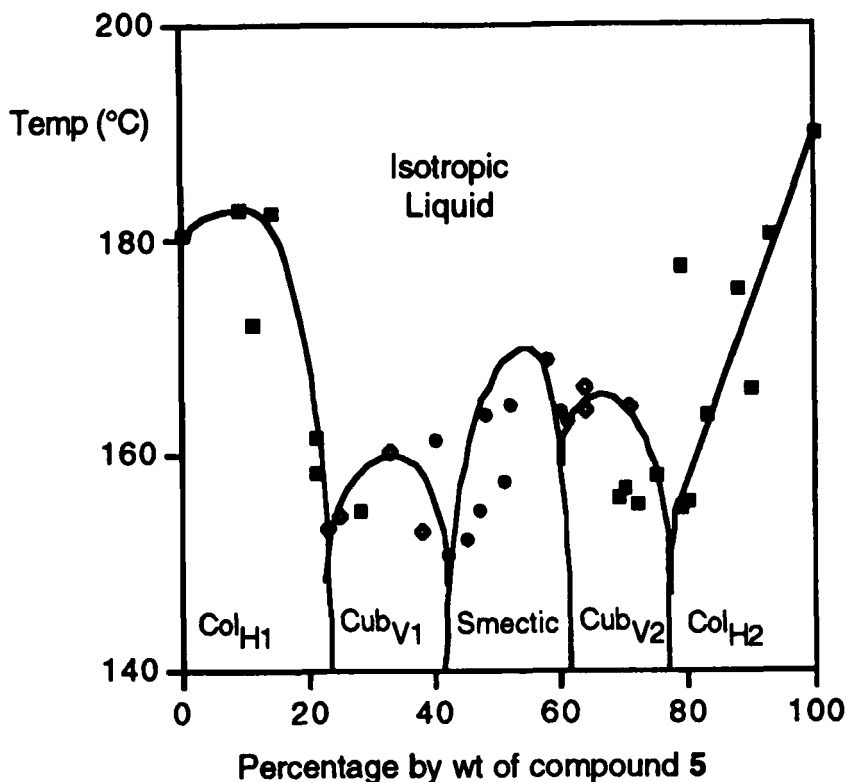
FIGURE 13 Miscibility phase diagram (wt %) as a function of temperature (°C) between compounds 5 (C14) and 6

decylamide with octadecanoyl D,L-dihydrogalactocerebroside, 7, see figure 12. We have shown previously that the dihydrogalactocerebroside exhibits a columnar phase[15], that has a structure with the polar head groups located towards the inner parts of the columns and the aliphatic chains in the outer regions. This material has a wedge-shaped molecular structure as depicted in the simulation shown in figure 12. Thus the head group is smaller in comparison to the cross-sectional areas of the aliphatic chains, which is the reverse of the relationship between the two in compound 5 (C14). It might be expected therefore that the two systems might induce opposite curvatures.

Figure 13 shows the phase diagram for binary mixtures of 5 (C14) and 6. It was found that as the phase diagram was traversed so columnar phases gave way to cubic, which in turn gave way to lamellar, the process was then repeated in reverse with lamellar giving cubic and cubic giving columnar. Thus induced cur-
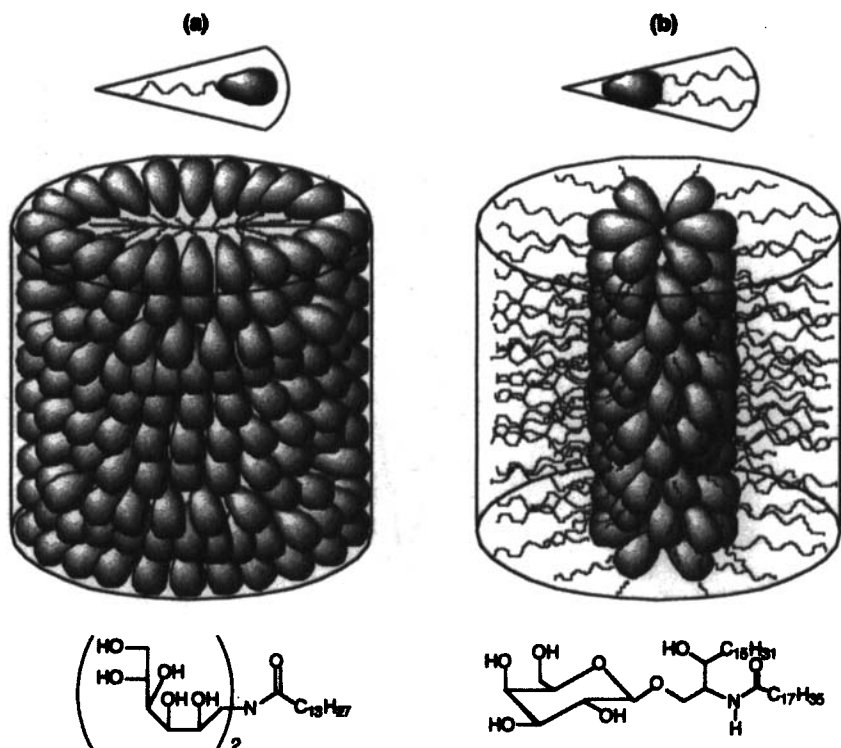
FIGURE 14 Comparison between columnar mesophases with positive and negative curvatures

vatures of the two compounds compensate for one another as a function of concentration. One material induces positive curvature whereas the other gives negative. The phase diagram therefore resembles that often obtained for lyotropic systems, as shown in figure 3. Similar results have been previously obtained by Borisch *et al* for polyhydroxy amphiphiles that exhibit columnar and cubic phases[16].

We can conclude from this study therefore that *N,N-bis-*(D-mannitolyl)tetradecylamide **5** (C14) exhibits a columnar phase where the polar head groups are located towards the outer surfaces of the column, whereas the aliphatic chains are located in the interior as shown in figure 14(a). This is the reverse of that found for octadecanoyl D,L-dihydrogalactocerebroside, **6**, see figure 14(b).

In conclusion we have shown that only by increasing the number of hydroxyl groups to around 4 to 5 in a bifurcated head group will we be able to induce the formation of a columnar phase. However, we know that two hydroxyl groups per

fork is insufficient for the formation of columnar phases and thus it would inter-esting to find the exact number OH groups that this change over takes place. Rigidity of the head group is found not to be capable of inducing a suitable degree of curvature for the tris systems studied. As with the bifurcated head group it will be necessary to increase the number of hydroxyl groups in trifur-cated head groups before columnar phases are formed.

Miscibility phase diagrams for thermotropic phases of poly-ols are capable of producing similar phase diagrams to those found for lyotropic systems as a func-tion of curvature. This unification of mesophase morphology between thermo-tropic and lyotropic phases shows that the two branches of liquid crystals (apart from the nematic phase) are dependent on curvature and microphase segregation in determining the type and nature of the phases that are formed[17,18].

Acknowledgements

References

1. K.J. Toyne, in *Thermotropic Liquid Crystals, Critical Reports on Applied Chemistry*, Vol 22, Ed G.W. Gray, Wiley, Chichester, 1987, pp 28–63.
2. J.W. Goodby, in the *Handbook of Liquid Crystals Vol 2A: Low Molecular Weight Liquid Crys-tals I*, Eds: D. Demus, J.W. Goodby, G.W. Gray, H.-W. Spiess and V. Vill, Wiley-VCH, Wein-heim, 1998, Ch V, pp 413–440.
3. A.W. Hall, J. Hollingshurst and J.W. Goodby, in the *Handbook of Liquid Crystal Research*, Eds P.J. Collings and J.S. Patel, Oxford University Press, New York and Oxford, 1997, pp 17–70.
4. J.W. Goodby, K.J. Toyne, M. Hird, P. Styring, R.A. Lewis, A. Beer, C.C. Dong, M.E. Glenden-ning, J.C. Jones, K.P. Lymer, A.J. Slaney, V. Minter and L.K.M. Chan, Proceedings of 12th Annual Symposium on Electronic Imaging of the IS&T/SPIE, San Jose, USA, 2000, and refer-ences therein.
5. H.T. Nguyen, C. Destrade and J. Malthête, in the *Handbook of Liquid Crystals Vol 2B: Low Molecular Weight Liquid Crystals II*, Eds: D. Demus, J.W. Goodby, G.W. Gray, H.-W. Spiess and V. Vill, Wiley-VCH, Weinheim, 1998, pp 865–900.
6. C. Tschierske, *J. Mater. Chem.*, **8**, 1485 (1998).
7. J.W. Goodby, J.A. Haley, M.J. Watson, G. Mackenzie, S.M. Kelly, P. Letellier, P. Godé, G. Goethals, G. Ronco, B. Harmouch, P. Martin and P. Villa, *Liq. Cryst.*, **22**, 497 (1997).
8. J.W. Goodby, M.J. Watson, G. Mackenzie, S.M. Kelly, S. Bachir, P. Bault, P. Godé, G. Goe-thals, P. Martin, G. Ronco and P. Villa, *Liq. Cryst.*, **25**, 139 (1998).
9. W.V. Dahlhoff, K. Radkowski, I. Dierking and P. Zugenmaier, *Z. Naturforsch*, **51b**, 1229 (1996).
10. J.W. Goodby, J.A. Haley, M.J. Watson, G. Mackenzie, S.M. Kelly, P. Letellier, O. Douillet, P. Godé, G. Goethals, G. Ronco and P. Villa, *Liq. Cryst.*, **22**, 367 (1997).
11. H.J.M. Kempen, C. Hoes, J.H. van Boom, H.H. Spanjer, J. de Lange, A. Langendoen and T.J.C. van Berhel, *J. Med. Chem.*, **27**, 1306 (1984).
12. CRC Handbook of Physics and Chemistry, ed R.C. Priest, CRC Press, Boca Raton, 68th Edi-tion, 1988.
13. J.W. Goodby, *Mol. Cryst. Liq. Cryst.*, **110**, 205 (1984); E. Barrall, B. Grant, M. Oxsen, E.T. Samulski, P.C. Moews, J.R. Knox, R.R. Gaskill and J.L. Haberfeld, *Org. Coat. Plast. Chem.*, **40**, 67 (1979).

14. G. Bonsergent, G. Mackenzie and D.F. Ewing, unpublished results, also see for example A. Coué, D.F. Ewing, J.W. Goodby, P. Letellier, G. Mackenzie and D. Plusquellec, *Carbohydr. Res.*, **300**, 341 (1997).
15. J.W. Goodby, *Liq. Cryst.*, **24**, 25 (1998).
16. K. Borisch, C. Tschierske, P. Göring and S. Diele, *Chem. Commun.*, 2711 (1998).
17. Y. Hendrikx and A.-M. Levelut, *Mol. Cryst. Liq. Cryst.*, **165**, 233 (1988).
18. A. Skoulios and D. Guillon, *Mol. Cryst. Liq. Cryst.*, **165**, 317 (1988).